Available online at www.sciencedirect.com

ScienceDirect

Physics Letters B 662 (2008) 302–308

PHYSICS LETTERS B

www.elsevier.com/locate/physletb

On the renormalization of the bosonized multi-flavor Schwinger model

I. Nándori

Institute of Nuclear Research of the Hungarian Academy of Sciences, H-4001 Debrecen, PO Box 51, Hungary

Received 26 July 2007; received in revised form 9 March 2008; accepted 9 March 2008

Available online 13 March 2008

Editor: L. Alvarez-Gaumé

Abstract

The phase structure of the bosonized multi-flavor Schwinger model is investigated by means of the differential renormalization group (RG) method. In the limit of small fermion mass the linearized RG flow is sufficient to determine the low-energy behavior of the N-flavor model, if it has been rotated by a suitable rotation in the internal space. For large fermion mass, the exact RG flow has been solved numerically. The low-energy behavior of the multi-flavor model is rather different depending on whether $N = 1$ or $N > 1$, where N is the number of flavors. For $N > 1$ the reflection symmetry always suffers breakdown in both the weak and strong coupling regimes, in contrary to the $N = 1$ case, where it remains unbroken in the strong coupling phase.

PACS: 11.10.Gh; 11.10.Hi; 11.10.Kk

Keywords: Renormalization group; Field theories in dimensions other than four

1. Introduction

Two-dimensional quantum electrodynamics (QED_2) or the Schwinger model [1] exhibits many analogies with four-dimensional quantum chromodynamics (QCD_4) including confinement, chiral condensate, topological θ-vacuum. The Lagrangian of QED_2 with massive N-flavor fermions which is called the N-flavor (or multi-flavor) Schwinger model reads [2–5]

$$\mathcal{L} = \sum_{n=1}^{N} \bar{\psi}_n \big(i\gamma^\mu \partial_\mu - m - g\gamma^\mu A_\mu\big)\psi_n - \frac{1}{4} F_{\mu\nu}F^{\mu\nu}, \tag{1}$$

where $F_{\mu\nu} = \partial_\mu A_\nu - \partial_\nu A_\mu$. Using bosonization technique [2–8] the fermionic theory (1) can be mapped onto an equivalent Bose form [2–5,8–19]

$$\mathcal{L} = N_m \left[\sum_{n=1}^{N} \frac{1}{2} (\partial_\mu \varphi_n)^2 + \frac{\mu^2}{2} \left(\sum_{n=1}^{N} \varphi_n \right)^2 - cm^2 \sum_{n=1}^{N} \cos\left(\sqrt{4\pi}\varphi_n - \frac{\theta}{N} \right) \right], \tag{2}$$

with $\mu^2 = g^2/\pi$, $c = e^\gamma/(2\pi)$ where $\gamma = 0.5774$ is the Euler's constant, θ is the vacuum angle parameter, N_m denotes normal-ordering w.r.t. m and φ_n $n = 1, \ldots, N$ are one-component scalar fields. Both the fermionic and the bosonic form of the model has been analyzed by various methods from various aspects, e.g. mass perturbation theory [12], density matrix renormalization group (RG) method [10], lattice calculations [10,14,15], momentum RG method [20], etc. Physical properties (like, e.g., chiral condensate [5,13,15–17], boson mass spectrum [14,16]) have been investigated for arbitrary values of θ, fermion mass and temperature.

The $(N = 1)$-flavor Schwinger model for $\theta = \pm\pi$ has two phases [3,9–12]. Illustrative and detailed analysis of the phase structure is presented in [11]. The behavior of the theory is controlled by dimensionless ratio g/m. For g/m large, i.e., for strong coupling, the symmetry $\varphi \leftrightarrow -\varphi$ is unbroken, there is a unique vacuum at $\varphi = 0$ and there are no half-asymptotic particles. For g/m small, i.e., for weak coupling, the reflection symmetry suffers spontaneous breakdown, there are two vacua

E-mail address: nandori@atomki.hu.

0370-2693
doi:10.1016/j.physletb.2008.03.011

approximately located at $\varphi = \pm\sqrt{\pi}/2$ and half-asymptotic particles appear.

The multi-flavor ($N \geqslant 2$) model has not been studied as extensively as the 1-flavor model. However, the relative ignorance toward the multi-flavor Schwinger model is perhaps not fully justified as it shows more resemblance to QCD_4, because the model features a chiral symmetry breakdown. Based on the study of chiral condensate [5,13,17,18], the behavior of the Schwinger model has been found to be distinctively different for $N = 1$ and for $N \geqslant 2$. Recently, the phase structure of the $(N = 1)$-flavor Schwinger model has been investigated by exact functional RG method [21] and it has been recovered in a rather straightforward way. Our aim in this work is to extend the RG analysis for the bosonized multi-flavor ($N \geqslant 2$) Schwinger model to consider its phase structure and clarify the difference between the 1-flavor and the multi-flavor models.

The multi-flavor Schwinger model has relevance in solid state physics, too. It has been used to describe antiferromagnetic spin chain (see, e.g., [22]) and the Bose form of the 1-flavor model has been proposed as an adequate model for the description of the vortex properties of two-dimensional (2D) isolated thin superconducting films [23] and the multi-flavor model has been used for description of vortex dynamics in magnetically coupled layered superconductors [24]. The number of flavors of the bosonized multi-flavor Schwinger model is equal to the number of layers of the superconducting layered system and the Fourier amplitude of the bosonic model (2) is related to the fugacity of the vortex gas. The RG techniques, like the real space RG method developed for spin systems usually rely on the dilute gas approximation which is equivalent to the linearized RG flow. However, in order to determine the phase structure and the vortex dynamics of layered systems in a reliable manner one has to incorporate the effect of the interlayer coupling which requires corrections to the dilute gas result. Our goal here is to show that the dilute gas approximation, i.e., the linearized RG flow, can be used to determine the phase structure of layered (multi-flavor) models in the limit of low fugacity (small fermion mass) if the original multi-layer (multi-flavor) model has been rotated in the internal space. For high fugacities (large fermion mass) one has to solve the exact RG flow numerically.

2. Multi-flavor models

The bosonized multi-flavor Schwinger model (2) can be considered as the specific form of a generalized multi-layer sine-Gordon (SG) model whose Euclidean action is written as

$$S = \int \mathrm{d}^2 r \left[\frac{1}{2} (\partial_\mu \underline{\varphi})(\partial_\mu \underline{\varphi})^{\mathrm{T}} + \frac{1}{2} \underline{\varphi}\, \underline{\underline{M}}^2 \underline{\varphi}^{\mathrm{T}} + \sum_{n=1}^{N} y_n \cos(b\varphi_n) \right], \tag{3}$$

with the $O(N)$ multiplet $\underline{\varphi} = (\varphi_1, \ldots, \varphi_N)$. For the specific choice, $b^2 = 4\pi$, and $\underline{\varphi}\, \underline{\underline{M}}^2 \underline{\varphi}^{\mathrm{T}} = \mu^2 (\sum_{n=1}^{N} \varphi_n)^2$, one recovers Eq. (2). The Fourier amplitude related to the fermion mass ($y \sim m$) and the exact relation can be determined by using normal-ordering w.r.t. the boson mass. The vacuum angle parameter has to be chosen as $\theta = \pm N\pi$ for $y_n > 0$ and $\theta = 0$ for $y_n < 0$. In general, SG-type models have also been successfully used to investigate vortex dynamics in 2D or quasi-2D superconductors [24,25]. Recently, it was shown in [24] that the LSG model with a suitable interlayer interaction,

$$\frac{1}{2} \underline{\varphi}\, \underline{\underline{M}}^2_{\text{M-LSG}} \underline{\varphi}^{\mathrm{T}} = \frac{1}{2} G \left(\sum_{n=1}^{N} a_n \varphi_n \right)^2, \tag{4}$$

can be used for magnetically coupled layered superconductors where the coupling strength between the layers denoted by G and $a_n = \pm 1$ are free parameters of the model. Based on symmetry considerations [24] any choice with $a_n^2 = 1$ should reproduce exactly the same phase structure, as a consequence, the Fourier amplitudes (i.e., fugacities) $y_n \equiv y$ for $n = 1, 2, \ldots, N$. The frequency b^2 is related inversely to the temperature of the corresponding solid-state system. Let us note that, different regions of the parameter space have to be considered for the condensed matter and for the high-energy physics problem. For the description of the multi-flavor Schwinger model, one should investigate the phase diagram in the two-dimensional plane $y - G$ (for $b^2 = 4\pi$) and for the vortex dynamics one has to consider the phase structure in terms of the frequency b^2. Let us note, the LSG model with magnetic type coupling has a single non-vanishing mass-eigenvalue $M_N^2 = NG$. Another definition for the mass term of Eq. (3)

$$\frac{1}{2} \underline{\varphi}\, \underline{\underline{M}}^2_{\text{J-LSG}} \underline{\varphi}^{\mathrm{T}} = \frac{1}{2} \sum_{n=1}^{N-1} J(\varphi_{n+1} - \varphi_n)^2, \tag{5}$$

is based on the discretization of the anisotropic 3D-SG model [26] which has been proposed as a suitable model for the vortex dynamics of Josephson coupled layered superconductors [27]. Although, it has been shown in [28], that the LSG model with the mass matrix (5) cannot be used for Josephson coupled layered superconductors, in order to distinguish between the two types of mass matrices, in this Letter we refer to (5) as the Josephson-type interlayer interaction. Let us note that the Josephson-type LSG model can also be considered as a bosonized version of an N-flavor fermionic model [26,29,30], but not that of the multi-flavor Schwinger model (1). In general, the LSG model with Josephson type coupling has a single zero and $N - 1$ non-zero mass-eigenvalues, therefore, the Josephson coupled LSG model is invariant under the particular exchange of the layers $\varphi_n \leftrightarrow \varphi_{N-n+1}$, hence, $y_n \equiv y_{N-n+1}$.

3. RG approach for multi-flavor models

In this section we summarize briefly the results of the RG analysis of LSG type models discussed in our previous publications [24,26,28–31] by means of the approximated form of the Wegner–Houghton [32] differential RG approach (WH–RG). The WH–RG method provides us the complete elimination of the modes in the Wilsonian RG method [33] above the moving momentum scale k which serves as a sharp cutoff. In principle any types of RG methods (see, e.g., [34]) can be used to consider the behavior of LSG type models. However, the usage of sharp momentum cutoff RG is reasonable since a spinodal instability [35,36] may occur during the flow [21,37–40] and this

can be used as a signature of spontaneous breakdown of the symmetry $\varphi \leftrightarrow -\varphi$. The WH–RG equation in the local potential approximation (LPA) for the LSG type models presented in Refs. [24,26,28–31] reads as

$$(2+k\partial_k)\tilde{V}_k(\underline{\varphi}) = -\frac{1}{4\pi}\ln\bigl[\det\bigl(\delta_{ij}+\tilde{V}_k^{ij}(\underline{\varphi})\bigr)\bigr], \tag{6}$$

where the dimensionless blocked potential $\tilde{V}_k = k^{-2}V_k$ is introduced and $\tilde{V}_k^{ij}(\underline{\varphi})$ denotes the second derivatives of the potential with respect to φ_i, φ_j. We make the following ansatz for the dimensionless blocked potential of the LSG type models

$$\tilde{V}_k(\underline{\varphi}) = \frac{1}{2}\underline{\varphi}\,\underline{\underline{\tilde{M}}}^2(k)\underline{\varphi}^{\mathrm{T}} + \sum_{n=1}^{N}\tilde{y}_n(k)\cos(b\varphi_n), \tag{7}$$

where $\tilde{y}_n(k) = k^{-2}y_n(k)$. Inserting the ansatz (7) into Eq. (6), the right-hand side becomes periodic, while the left-hand side contains both periodic and non-periodic parts [26,29–31]. The non-periodic part contains only mass terms, so that we obtain a trivial tree-level RG flow equation for the dimensionless mass matrix $(2+k\partial_k)\underline{\underline{\tilde{M}}}^2(k) = 0$, which provides the trivial scaling $\tilde{J}_k = k^{-2}J$ and $\tilde{G}_k = k^{-2}G$, where the dimensionful interlayer couplings J, G remain constant during the blocking. Finally, we recall that in LPA there is no wave-function renormalization, thus the parameter b also remains constant during the blocking. The argument of the logarithm in Eq. (6) must be positive. If the argument vanishes or if it changes sign at a critical value k_{SI}, the WH–RG equation (6) loses its validity for $k < k_{\mathrm{SI}}$. This is a consequence of the spinodal instability (SI) [35,36]. Below the critical scale $k < k_{\mathrm{SI}}$ the tree-level blocking relation (see Eq. (13) of [31]) can be used to determine the RG flow. In this Letter we do not investigate the tree-level RG flow of LSG type models but we use the appearance of the spinodal instability as a signature of the spontaneous breakdown of the reflection symmetry.

In general, the solution of Eq. (6) can only be obtained numerically, however, various approximations of Eq. (6) are also available in Refs. [26,28–31]. We compare two types of approximations, the dilute gas result which is equivalent to the linearized RG and the mass-corrected RG flow which incorporates the mass term correctly and is able to provide the phase structure of the LSG type models in a reliable manner. The linearization of the WH–RG equation (6) in the full potential around the UV Gaussian fixed point [41] by assuming $|\partial_{\varphi_i}^2\tilde{V}_k| \ll 1$,

$$(2+k\partial_k)\tilde{V}_k(\underline{\varphi}) \approx -\frac{1}{4\pi}\sum_{n=1}^{N}\tilde{V}_k^{nn}(\underline{\varphi}), \tag{8}$$

for the ansatz (7) leads to the linearized WH–RG flow [31] exhibiting the solutions

$$\tilde{y}_n(k) = \tilde{y}_n(\Lambda)\left(\frac{k}{\Lambda}\right)^{-2+\frac{b^2}{4\pi}}, \tag{9}$$

where $\tilde{y}_n(\Lambda)$ are the initial (bare) values of the fugacities at the high energy ultra-violet (UV) cutoff Λ. These are the scaling laws valid at the asymptotically large UV scales ($k \sim \Lambda$), and being independent of the interlayer coupling (i.e., mass terms) predicting a phase structure very similar to that of the massless 2D-SG model [37,42]. The critical frequency $b_c^2 = 8\pi$ separates the two phases of the model [6] and the critical temperature is related inversely to the critical frequency $T^{\star}_{\mathrm{KTB}} \sim 1/b_c^2$ [35,37,41]. Let us note that the linearized WH–RG equations obtained in LPA for the $(N=2)$-layer LSG model, are the same as those have been found in [27] in the dilute gas approximation except of the loss of the scale-dependence of b due to the usage of the LPA [31]. The couplings $\tilde{J}_k$ and $\tilde{G}_k$ are always a relevant parameters in the LSG models and, consequently, the linearization, i.e., the asymptotic UV scaling law (9), loses its validity with decreasing scale k for any value of b.

The simplest way to go beyond the linearized (i.e., the dilute gas) approximation and to improve the extrapolating power of the UV scaling laws is to take corrections into account of the order $\mathcal{O}(J/k^2)$ for the Josephson and $\mathcal{O}(G/k^2)$ for the magnetic case, which results in the mass-corrected UV scaling laws derived for the LSG model in Refs. [24,26,29]. This is achieved by linearizing the WH–RG equation in the periodic piece of the blocked potential,

$$(2+k\partial_k)\tilde{U}_k(\varphi_1,\ldots,\varphi_N) \approx -\frac{1}{4\pi}\frac{F_1(\tilde{U}_k)}{C}, \tag{10}$$

where $\tilde{U}_k(\varphi_1,\ldots,\varphi_N) = \sum_{n=1}^{N}\tilde{y}_n(k)\cos(b\varphi_n)$ and C and $F_1(\tilde{U}_k)$ stand for the constant and linear pieces of the determinant $\det[\delta_{ij}+\tilde{V}_k^{ij}] \approx C + F_1(\tilde{U}_k) + \mathcal{O}(\tilde{U}_k^2)$. Let us first determine the mass-corrected UV scaling laws for the LSG model with Josephson type interlayer interaction for $N=2$. In this case the solution of Eq. (10) is [26,29]

$$\tilde{y}(k) = \tilde{y}(\Lambda)\left(\frac{k}{\Lambda}\right)^{\frac{b^2}{8\pi}-2}\left(\frac{k^2+2J}{\Lambda^2+2J}\right)^{\frac{b^2}{16\pi}}, \tag{11}$$

with the initial value $\tilde{y}(\Lambda)$ at the UV cutoff $k=\Lambda$. From the extrapolation of the UV scaling law Eq. (11) to the IR limit, we can read off the critical values $b_c^2 = 16\pi$, for $N=2$. The coupling $\tilde{y}$ is irrelevant for $b^2 > b_c^2$ and relevant for $b^2 < b_c^2$. The general expressions for the critical frequency and the corresponding critical temperature [28] read

$$b_c^2(N) = 8\pi N \quad\rightarrow\quad T^{(N)}_{\text{J-LSG}} = \frac{2\pi}{b_c^2(N)} = T^{\star}_{\mathrm{KTB}}\frac{1}{N}, \tag{12}$$

which are determined previously in a similar manner in the framework of the rotated LSG model in Refs. [26,29,30]. The presence of the coupling J between the layers modifies the critical parameter b_c^2 of the Josephson coupled LSG model as compared to the massless 2D-SG model. This important modification can only be deduced if one goes beyond the linearized (i.e., dilute gas) approximation, e.g., by the usage of the mass-corrected UV scaling laws. The similar consideration can be done for the LSG model with magnetic type coupling [24,29]. Since the layers are assumed to be equivalent for the magnetically coupled LSG model, the RG flow equations for the fugacities of different layers should be the same ($\tilde{y}_n(k) \equiv \tilde{y}(k)$)

and the solution can be obtained analytically

$$\tilde{y}(k) = \tilde{y}(\Lambda)\left(\frac{k}{\Lambda}\right)^{\frac{(N-1)b^2}{N4\pi}-2}\left(\frac{k^2+NG}{\Lambda^2+NG}\right)^{\frac{b^2}{N8\pi}}, \tag{13}$$

where $\tilde{y}(\Lambda)$ is the initial value for the fugacity at the UV cutoff Λ and G, b^2 are scale-independent parameters. The critical frequency and the corresponding critical temperature which separates the two phases of the model can be read directly

$$b_c^2(N) = \frac{8\pi N}{N-1} \quad \rightarrow \quad T^{(N)}_{\text{M-LSG}} = \frac{2\pi}{b_c^2(N)} = T^{\star}_{\text{KTB}}\frac{N-1}{N}. \tag{14}$$

For $N \to \infty$ the magnetically coupled LSG behaves like a massless 2D-SG model with the critical frequency $b_c^2 = 8\pi$. In principle, one can try to determine the phase structure of the LSG models relying on the dilute gas approximation as it has been discussed in Ref. [43] for the 2-layer model. However, in this case a 2-stages RG procedure is required. In the first step, the real space RG equations are integrated out from the UV cutoff ($a_0 \sim 1/\Lambda$) to the effective screening length $\lambda_{\text{eff}} = 1/\sqrt{2G} = 1/\sqrt{2J}$, where the topological defects are taken into account with full flux. In the second RG step, from λ_{eff} to infinity, an a priori assumption has been done by introducing topological excitations with fractional flux and, consequently, the predicting power of the RG approach has been weakened. In the next sections we show that after an appropriate rotation of layered models in the internal space, the dilute gas RG results can be used to determine the phase structure of LSG type models without using any a priori assumptions.

4. RG analysis for rotated models

After performing an $O(N)$ rotation of the layered models which diagonalizes the mass matrix, the rotated models do not have interlayer interactions, consequently, the rotated fields can be treated separately. Let us note that the rotation has generally been used for coupled two-dimensional models, e.g., for the SU(N) Thirring model [5] and for the 2-flavor [3,4,14,15] and for the N-flavor Schwinger models [8,13,17,18]. The details of the rotation of the N-layer Josephson coupled LSG model has also been discussed in Refs. [26,30]. Depending on the number of the non-trivial mass eigenvalues, some of the rotated fields have explicit mass terms (massive modes) and the other ones are massless, SG-type fields [3,4,17]. For example, the dimensionless potential of the rotated Josephson coupled LSG model contains $N-1$ massive fields

$$\tilde{V}_{\text{J-rot}} = \sum_{n=2}^{N}\frac{1}{2}\tilde{M}_n^2\alpha_n^2 + \sum_{\sigma_1,\ldots,\sigma_N}\tilde{w}_{\sigma_1,\ldots,\sigma_N}\prod_{n=1}^{N}e^{i\sigma_n b_n\alpha_n}, \tag{15}$$

with the rotated $O(N)$ multiplet $\underline{\alpha}^T = \underline{\underline{O}}^T\underline{\varphi}^T$ where $\underline{\underline{O}}$ represents the rotation with $b_1^2 = b^2/N$, $b_{n>1}^2 = b^2/(n(n-1))$ and the integer valued σ_n represent the charges of the topological excitations. The rotated magnetic-type LSG model consists of a single massive field

$$\tilde{V}_{\text{M-rot}} = \frac{1}{2}\tilde{M}^2\alpha_1^2 + \sum_{\sigma_1,\ldots,\sigma_N}\tilde{w}_{\sigma_1,\ldots,\sigma_N}\prod_{n=1}^{N}e^{i\sigma_n b_n\alpha_n}, \tag{16}$$

where $M^2 = NG$ and the amplitudes $w_{\sigma_1,\ldots,\sigma_N}$ are different for the Josephson and magnetic LSG models. At low energies, below the mass-scale the quantum fluctuations are suppressed by the mass terms producing a trivial scaling for the massive modes [41], so, the massive modes can be considered perturbatively [30,41] and they do not influence the phase structure of the rotated models. Therefore, one should only consider the remaining massless SG fields in order to determine the phases of the layered system. At the lowest order of the perturbation theory, all the massive modes are set to be equal to zero. In this case the effective potential for the rotated Josephson type LSG model reads as

$$\tilde{V}_{\text{J-rot}}(\alpha_1) = \sum_{\sigma_1}\tilde{w}_{\sigma_1}e^{i\sigma_1 b_1\alpha_1}, \tag{17}$$

and for the magnetically coupled LSG model the effective potential is

$$\tilde{V}_{\text{M-rot}}(\alpha_2,\ldots,\alpha_N) = \sum_{\sigma_2,\ldots,\sigma_N}\tilde{w}_{\sigma_2,\ldots,\sigma_N}\prod_{n=2}^{N}e^{i\sigma_n b_n\alpha_n}. \tag{18}$$

Let us consider the fundamental modes $\sigma_n = \pm 1$. The linearized WH–RG equation (8) with $\tilde{V}_k^{nn} = \partial_{\alpha_n}^2\tilde{V}_k$, for the ansatz (17) and (18) leads to the linearized RG flow equations

$$\begin{aligned}(2+k\partial_k)\tilde{w}_{\text{J}}(k) &= \frac{b_1^2}{4\pi}\tilde{w}_{\text{J}}(k),\\ (2+k\partial_k)\tilde{w}_{\text{M}}(k) &= \frac{1}{4\pi}\left(\sum_{n=2}^{N}b_n^2\right)\tilde{w}_{\text{M}}(k),\end{aligned} \tag{19}$$

exhibiting the solutions

$$\begin{aligned}\tilde{w}_{\text{J}}(k) &= \tilde{w}_{\text{J}}(\Lambda)\left(\frac{k}{\Lambda}\right)^{-2+\frac{b^2}{N(4\pi)}},\\ \tilde{w}_{\text{M}}(k) &= \tilde{w}_{\text{M}}(\Lambda)\left(\frac{k}{\Lambda}\right)^{-2+\frac{(N-1)b^2}{N(4\pi)}},\end{aligned} \tag{20}$$

where $\tilde{w}_{\text{J}}(\Lambda)$ and $\tilde{w}_{\text{M}}(\Lambda)$ are the initial values for the Fourier amplitudes at the high energy UV cutoff Λ. The critical value of the frequency parameter and the corresponding critical temperatures are found to be equivalent to Eq. (12) for the Josephson and Eq. (14), for the magnetic case. Consequently, the dilute gas RG results for the rotated models predict the same layer-dependence of the critical temperature as that of obtained by the mass-corrected RG for the original LSG-type models. This proves that the dilute gas approximation is suitable to determine the phase structure of rotated layered systems for low fugacities. However, for $b^2 < b_c^2$, the fugacities $\tilde{y}_n$ are increasing parameters, consequently, only the exact RG flow is able to determine the phase structure of the LSG-type models in a reliable manner.

5. Exact RG flow for the ($N = 2$)-flavor model

Since the results (12) and (14) have been established by an UV approximated RG method, it is certainly worthwhile to confirm the analysis by a numerical calculation of the exact

RG flow. Moreover, if one considers the appearance or non-appearance of spinodal instability during the blocking which can be used as a signature of spontaneous symmetry breakdown of the reflection symmetry, the numerical solution of the exact WH–RG equation is required. Indeed, the full RG analysis of the 1-layer LSG model at $b^2 = 4\pi$ discussed in Ref. [21] provides us the tool to investigate the symmetric and the symmetry broken phases of the 1-flavor massive Schwinger model. The critical value of the ratio $(\frac{m}{g})_c = 0.311$ which separates the two phases of the 1-flavor model has been determined by the exact RG method which coincides with the results of other calculations (see, e.g., [10]). If $g \gg m$, i.e., below the critical ratio, the spinodal instability does not appear during the RG flow, therefore, the reflection symmetry remains unbroken. This is the consequence of the trivial scaling of the Fourier amplitudes below the mass-scale. However, for $g \ll m$, i.e., above the critical value, the spinodal instability always appears. One may assume a similar phase structure for the multi-layer model, however, it has been argued in the literature [8,13,17] that the low-energy behavior of the multi-flavor Schwinger model is different depending on whether $N = 1$ or $N \geqslant 2$. Our aim here is to clarify this issue by the numerical solution of the exact WH–RG equation derived for the 2-layer LSG model. We will show that spinodal instability always appears for the 2-layer LSG model for $b^2 = 4\pi$.

We determine numerically the dimensionless effective potential $\tilde{V}_{\rm eff}(\varphi_1, \varphi_2)$ for the double-layer LSG model as the limit $k \to 0$ of the dimensionless blocked potential

$$\tilde{V}_k(\varphi_1, \varphi_2) = \frac{1}{2}\tilde{G}_k(\varphi_2 - \varphi_1)^2 + \tilde{U}_k(\varphi_1, \varphi_2), \tag{21}$$

where $\tilde{U}_k(\varphi_1, \varphi_2)$ is an arbitrary periodic function of the fields (with Z_2 symmetry) including all the Fourier modes generated during the RG flow. In order to consider the effect of the higher Fourier modes, which were not taken into account in the previously utilized linearized and mass-corrected linearized WH–RG approach, we use the following ansatz for periodic part of the blocked potential

$$\tilde{U}_k = \tilde{u}_{01}(k)\big[\cos(b\varphi_1) + \cos(b\varphi_2)\big] + \tilde{u}_{11}(k)\cos(b\varphi_1)\cos(b\varphi_2) + \tilde{v}_{11}(k)\sin(b\varphi_1)\sin(b\varphi_2), \tag{22}$$

with the fundamental mode $\tilde{u}_{01} = \tilde{u}_{10} = \tilde{y}$. Inserting the ansatz (21) into the exact WH–RG equation (6) and separating the periodic and non-periodic parts, one arrives at the RG equation for the periodic part, see Eq. (17) of Ref. [31]. For technical reasons, it is more convenient to consider derivative of the WH–RG equation with respect to one of the field variables. By Fourier decomposition, this RG equation can be reduced to a set of ordinary differential equations for the couplings $\tilde{u}_{01}$, $\tilde{u}_{11}$ and $\tilde{v}_{11}$,

$$\underline{\underline{A}}\begin{pmatrix} D_k\tilde{u}_{01} \\ D_k\tilde{u}_{11} \\ D_k\tilde{v}_{11} \end{pmatrix} = \frac{b^2}{4\pi}\begin{pmatrix} -2(1+\tilde{G})\tilde{u}_{01} + b^2\tilde{u}_{01}\tilde{u}_{11} \\ -2(1+\tilde{G})\tilde{u}_{11} + 2\tilde{G}\tilde{v}_{11} + b^2\tilde{u}_{11}^2 \\ -2(1+\tilde{G})\tilde{v}_{11} + 2\tilde{G}\tilde{u}_{11} \end{pmatrix}, \tag{23}$$

where $D_k \equiv (2 + k\partial_k)$ and element of the matrix $\underline{\underline{A}}$ are $\underline{\underline{A}}_{11} = -2(1+2\tilde{G}) + \frac{b^4}{2}(\tilde{u}_{11}^2 - \tilde{v}_{11}^2)$, $\underline{\underline{A}}_{22} = \underline{\underline{A}}_{33} = -(1+2\tilde{G})$, $\underline{\underline{A}}_{12} = \underline{\underline{A}}_{21} = b^2(1+\tilde{G})\tilde{u}_{01} - \frac{b^4}{4}\tilde{u}_{01}\tilde{u}_{11}$, $\underline{\underline{A}}_{13} = \underline{\underline{A}}_{31} = \frac{b^4}{4}\tilde{u}_{01}\tilde{v}_{11}$, and $\underline{\underline{A}}_{23} = \underline{\underline{A}}_{32} = 0$. We invert the matrix $\underline{\underline{A}}$ and solve the RG flow equations for the Fourier amplitudes $\tilde{u}_{01}$, $\tilde{u}_{11}$ and $\tilde{v}_{11}$ numerically, by a fourth order Runge–Kutta method, whose numerical stability was verified by varying the step size. The main advantage of the numerical solution of the WH–RG flow equation (23) is that all the non-linear terms are kept. The numerically determined scaling of the couplings $\tilde{u}_{01}(k)$, $\tilde{u}_{11}(k)$ and $\tilde{v}_{11}(k)$ can be compared to the corresponding approximate UV scaling laws. The results are the followings. The mass-corrected UV scaling law (10) for the fundamental mode (u_{01}) coincides with the numerically obtained one. For the example, for $b^2 = 12\pi$, the deviation between the numerical solution of the exact WH–RG equation and the solution of the mass-corrected UV linearized WH–RG equation at the scale $k = 1.0 \times 10^{-5}$ is 9.69×10^{-7}. This coincidence demonstrates that the flow of the fundamental coupling $\tilde{u}_{01}$ is well described by the mass-corrected UV scaling law if no spinodal instability appears during the blocking. Therefore, we find that for low fugacities (small fermion mass), the phase structure of the double-layer LSG model obtained numerically is the same as that predicted by the extrapolation of the mass-corrected UV scaling laws, because the higher harmonics do not modify the scaling of the fundamental mode (see Figs. 1 and 2). The IR behavior of the higher harmonics and consequently the effective potential can only be determined by the numerical solution of the exact WH–RG equation when all the non-linear terms are kept. For example, the UV approximated RG flow is not able to determine the sign changes (see the peaks of the dotted and dashes lines in the figures) of the higher harmonics. According to the exact RG flow, in the IR limit u_{11} and v_{11} coincide independently of their initial values at the UV cutoff (see Fig. 2). Therefore, the low-energy effective potential of the 2-layer LSG model determined by the exact RG approach is

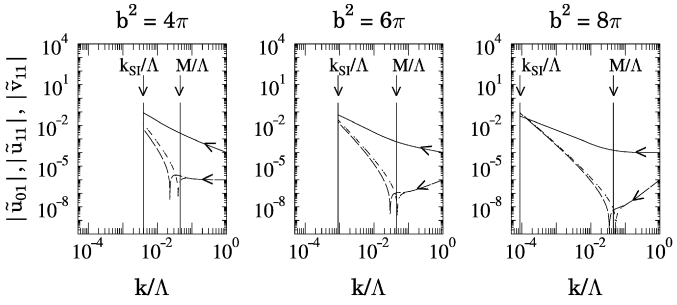

Fig. 1. The exact RG scaling of the dimensionless coupling constants $\tilde{u}_{01}$, $\tilde{u}_{11}$ and $\tilde{v}_{11}$ of the double-layer LSG model is represented graphically for various frequency parameters. The mass scale is $M/\Lambda = \sqrt{0.002}$. The full, dotted and dashed lines correspond to $\tilde{u}_{01}, \tilde{u}_{11}$ and $\tilde{v}_{11}$ respectively. Spinodal instability ($k_{\rm SI}/\Lambda$) appears below the mass scale. For increasing value of b^2 the momentum scale $k_{\rm SI}$ tends to zero and vanishes at $b^2 = 16\pi$. Below $k_{\rm SI}$ the WH–RG equation (6) looses its validity and the tree-level RG relation (Eq. (13) of [31]) has to be used which is not discussed here.

$$\tilde{V}_{\rm eff} = \frac{\tilde{G}}{2}(\varphi_2 - \varphi_1)^2 + \tilde{u}_{01}\big[\cos(b\varphi_1) + \cos(b\varphi_2)\big] + \tilde{w}_{11}\cos(b\varphi_1 - b\varphi_2), \tag{24}$$

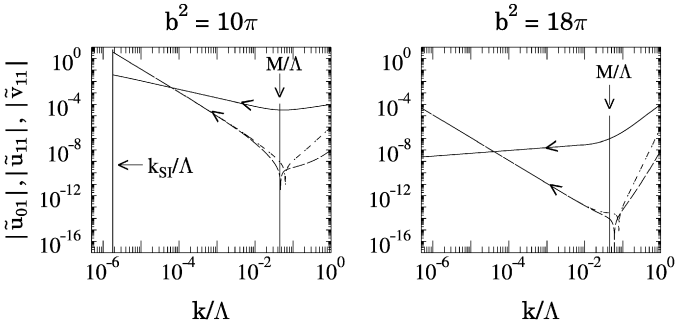

Fig. 2. The scaling of the dimensionless coupling constants of the double-layer LSG model is shown for two different frequencies $b^2 = 10\pi$ and $b^2 = 18\pi$ and for the mass scale $M/\Lambda = \sqrt{0.002}$. The UV ($M \ll k$) and IR ($k \ll M$) regions are separated by the mass eigenvalue. The scaling of the fundamental mode $\tilde{u}_{01}$ (full line) depends on the frequency, increasing (relevant) for $b^2 < 16\pi$ and decreasing (irrelevant) for $b^2 > 16\pi$. The initial values and consequently the UV scalings are different for $\tilde{u}_{11}$ (dotted) and $\tilde{v}_{11}$ (dashed) but in the IR region the trajectories are coincides resulting in a trivial tree-level scaling ($\sim k^{-2}$) which is independent of the frequency.

with $\tilde{w}_{11} \equiv \tilde{u}_{11} = \tilde{v}_{11}$ which corresponds to the massive mode in the rotated form of the model, hence, w_{11} has a trivial tree-level IR scaling ($\sim k^{-2}$) which is independent of the frequency b^2. The numerical solution of the exact WH–RG equation shows (Fig. 1) that for the 2-layer LSG model with $b^2 = 4\pi$, the spinodal instability (SI) always appears during the RG flow in contrary to the 1-layer model where the appearance of SI can be avoided for sufficiently small initial value for the fugacity. For the 1-flavor model for low fugacity, the SI cannot be detected below the mass scale since the presence of the mass term predicts a trivial tree-level scaling for all the Fourier amplitudes. For the 2-flavor model, below the mass scale, only the massive modes have trivial scalings but not for the fundamental one (u_{01}). Hence, the appearance of SI is unavoidable.

6. Summary

In this Letter we investigated the phase structure and the low-energy behavior of the bosonized multi-flavor Schwinger model (2) by means of the Wegner–Houghton RG method. The Bose form of the multi-flavor model consists of 2D sine-Gordon fields coupled by an appropriate mass matrix (4) which has also been used to describe the vortex properties of magnetically coupled layered superconductors [24]. Another definition (see Eq. (5)) for the mass matrix of the multi-flavor, i.e., layered sine-Gordon model has also been discussed which is based on discretization of the 3D sine-Gordon model [26]. Let us note, that the layered model with the mass matrix (5) can in principle also be considered as a Bose form of a fermionic model as it has been argued in [26,30], however not that of the multi-flavor Schwinger model (1).

It has been shown that in the limit of small fermion mass the linearized RG flow (i.e., the dilute gas approximation) is sufficient to determine the phase structure of the multi-flavor model in a reliable manner, if it has been rotated by a suitable rotation in the internal space which diagonalizes the mass matrix. This receives important application in condensed matter physics where the usual RG techniques are based on the dilute gas approximation. For example, using the idea of rotation the vortex dynamics of magnetically coupled layered superconductors can be considered by means of dilute gas RG methods and no two-stages RG [43] is required. The calculation of the exact Wegner–Houghton RG flow of the 2-flavor (i.e., 2-layer) layered sine-Gordon model, by a numerical approach including higher-order Fourier modes confirms that the mass-corrected UV scaling law (i.e., the linearized RG flow for the rotated model) is sufficient to determine the phase structure of the layered sine-Gordon model in the low fugacity (small fermion mass) limit.

The rigorous RG study of the layered sine-Gordon model verifies that the low energy effective potential of the bosonized multi-flavor Schwinger model is a sine-Gordon type model which undergoes a KTB-type phase transition at the flavor-number dependent critical frequency $b_c^2(N) = 8\pi N/(N-1)$. In the limit $N \to \infty$, the layered sine-Gordon model tends to the two-dimensional sine-Gordon theory with the critical frequency $b_c^2 = 8\pi$. Therefore, in the large N limit, the low energy behavior of the bosonized multi-flavor Schwinger model becomes independent of the boson mass, i.e., the coupling g. This is consistent with the flavor-dependence of the chiral condensate $\langle\bar{\psi}, \psi\rangle \sim m^{(N-1)/(N+1)} g^{2/(N+1)}$, and the mass gap $M_{\text{gap}} \sim m^{N/(N+1)} g^{1/(N+1)}$ which are independent of g if $N \to \infty$ [17]. The numerical solution of the exact RG equation shows that in case of the 2-flavor (i.e., 2-layer) layered sine-Gordon model with $b^2 = 4\pi$, the spinodal instability always appear during the RG flow in contrary to the 1-layer model where the appearance of spinodal instability can be avoided for sufficiently small initial value for the fugacity. Consequently, for $N > 1$ the reflection symmetry always suffers breakdown in both the weak and strong coupling regimes, in contrary to the $N = 1$ case, where it remains unbroken in the strong coupling phase.

Finally, let us mention that the extension of the RG analysis presented in this Letter can also be used to consider the θ-dependence of the multi-flavor model and to map out the phase structure of the multi-frequency sine-Gordon type models [44].

Acknowledgements

The author acknowledges the numerous fruitful discussions with U.D. Jentschura, S. Nagy, K. Sailer, K. Vad and the warm hospitality during a visit to the Max–Planck–Institute for Nuclear Physics (Heidelberg).

References

[1] J. Schwinger, Phys. Rev. 128 (1962) 2425.
[2] S.R. Coleman, R. Jackiw, L. Susskind, Ann. Phys. 93 (1975) 267.
[3] S.R. Coleman, Ann. Phys. 101 (1976) 239.
[4] W. Fischler, J. Kogut, L. Susskind, Phys. Rev. D 19 (1979) 1188.
[5] M.B. Halpern, Phys. Rev. D 13 (1976) 337.
[6] S.R. Coleman, Phys. Rev. D 11 (1975) 2088.
[7] M.B. Halpern, Phys. Rev. D 12 (1975) 1684.
[8] D. Gepner, Nucl. Phys. B 252 (1985) 481.
[9] Wen-Fa Lu, Phys. Rev. D 59 (1999) 105021;

Wen-Fa Lu, J. Phys. G 26 (2000) 1187.
[10] T.M. Byrnes, P. Sriganesh, R.J. Bursill, C.J. Hammer, Nucl. Phys. B (Proc. Suppl.) 109 (1) (2002) 202;
T.M. Byrnes, P. Sriganesh, R.J. Bursill, C.J. Hammer, Phys. Rev. D 66 (2002) 013002.
[11] R. Shankar, G. Murthy, cond-mat/0508242.
[12] C. Adam, Phys. Lett. B 382 (1996) 383;
C. Adam, Phys. Lett. B 382 (1996) 111;
C. Adam, Phys. Lett. B 440 (1998) 117;
C. Adam, Phys. Lett. B 555 (2003) 132.
[13] J.E. Hetrick, Y. Hosotani, S. Iso, Phys. Lett. B 350 (1995) 92;
R. Rodriguez, Y. Hosotani, Phys. Lett. B 375 (1996) 273;
Y. Hosotani, R. Rodriguez, Phys. Lett. B 389 (1996) 121;
Y. Hosotani, R. Rodriguez, J. Phys. A 31 (1998) 9925.
[14] C. Gattringer, I. Hip, C.B. Lang, Phys. Lett. B 466 (1999) 287.
[15] S. Häusler, C.B. Lang, Phys. Lett. B 515 (2001) 213;
H. Fukaya, T. Onogi, Phys. Rev. D 68 (2003) 074503;
H. Fukaya, T. Onogi, Phys. Rev. D 70 (2004) 054508.
[16] M. Creutz, Nucl. Phys. B (Proc. Suppl.) 42 (1995) 56;
M. Creutz, Rev. Mod. Phys. 73 (2001) 119;
M. Creutz, Ann. Phys. 321 (2006) 2782.
[17] A.V. Smilga, Phys. Rev. D 55 (1997) 443;
A.V. Smilga, Phys. Lett. B 278 (1992) 371.
[18] I. Affleck, Nucl. Phys. B 265 (1986) 448.
[19] S. Nagy, J. Polonyi, K. Sailer, Phys. Rev. D 70 (2004) 105023;
S. Nagy, J. Polonyi, K. Sailer, Acta Phys. Hung. A 19 (3–4) (2004) 247;
S. Nagy, K. Sailer, Philos. Mag. B 81 (2001) 1583.
[20] I. Ichinose, H. Mukaida, Int. J. Mod. Phys. A 9 (1994) 1043.
[21] S. Nagy, I. Nándori, J. Polonyi, K. Sailer, Phys. Rev. D 77 (2008) 025026.
[22] Y. Hosotani, J. Phys. A: Math. Gen. 30 (1997) L757;
F. Berruto, G. Grignani, G.W. Semenoff, P. Sodano, Ann. Phys. 275 (1999) 254.
[23] S.W. Pierson, O.T. Valls, Phys. Rev. B 61 (2000) 663.
[24] I. Nándori, K. Vad, S. Mészáros, U.D. Jentschura, S. Nagy, K. Sailer, J. Phys.: Condens. Matter 19 (2007) 496211.
[25] L. Benfatto, C. Castellani, T. Giamarchi, Phys. Rev. Lett. 98 (2007) 117008;
L. Benfatto, C. Castellani, T. Giamarchi, Phys. Rev. Lett. 99 (2007) 207002.
[26] I. Nándori, J. Phys. A: Math. Gen. 39 (2006) 8119.
[27] S.W. Pierson, O.T. Valls, Phys. Rev. B 45 (1992) 13076;
S.W. Pierson, O.T. Valls, H. Bahlouli, Phys. Rev. B 45 (1992) 13035.
[28] I. Nándori, U.D. Jentschura, S. Nagy, K. Sailer, K. Vad, S. Mészáros, J. Phys.: Condens. Matter 19 (2007) 236226.
[29] I. Nándori, S. Nagy, K. Sailer, U.D. Jentschura, Nucl. Phys. B 725 (2005) 467.
[30] U.D. Jentschura, I. Nándori, J. Zinn-Justin, Ann. Phys. 321 (2006) 2647.
[31] I. Nándori, K. Sailer, Philos. Mag. 86 (2006) 2033.
[32] F.J. Wegner, A. Houghton, Phys. Rev. A 8 (1973) 401.
[33] K.G. Wilson, Phys. Rev. D 3 (1971) 1818.
[34] J. Polchinski, Nucl. Phys. B 231 (1984) 269;
C. Wetterich, Phys. Lett. B 301 (1993) 90;
T.R. Morris, Int. J. Mod. Phys. A 9 (1994) 2411;
J. Comellas, Nucl. Phys. B 509 (1998) 662;
M.E. Fisher, Rev. Mod. Phys. 70 (1998) 653;
D.F. Litim, J. Pawlowski, The Exact Renormalization Group, World Scientific, 1999, p. 168;
D.F. Litim, Phys. Lett. B 486 (2000) 92;
C. Bagnuls, C. Bervillier, Phys. Rep. 348 (2001) 91;
J. Alexandre, J. Polonyi, Ann. Phys. 288 (2001) 37;
J. Berges, N. Tetradis, C. Wetterich, Phys. Rep. 363 (2002) 223;
J. Pawlowski, Ann. Phys. 322 (2007) 2831;
H. Gies, hep-th/0611146.
[35] J. Polonyi, Central Eur. J. Phys. 1 (2004) 1.
[36] J. Alexandre, V. Branchina, J. Polonyi, Phys. Lett. B 445 (1999) 153.
[37] I. Nándori, J. Polonyi, K. Sailer, Phys. Rev. D 63 (2001) 045022;
I. Nándori, J. Polonyi, K. Sailer, Philos. Mag. B 81 (2001) 1615.
[38] I. Nándori, K. Sailer, U.D. Jentschura, G. Soff, Phys. Rev. D 69 (2004) 025004;
I. Nándori, K. Sailer, U.D. Jentschura, G. Soff, J. Phys. G 28 (2002) 607.
[39] S. Nagy, I. Nándori, J. Polonyi, K. Sailer, Phys. Lett. B 647 (2007) 152.
[40] S. Nagy, K. Sailer, J. Polonyi, J. Phys. A 39 (2006) 8105.
[41] J. Zinn-Justin, Quantum Field Theory and Critical Phenomena, Clarendon Press, Oxford, 1996.
[42] D. Amit, Y.Y. Goldschmidt, G. Grinstein, J. Phys. A 13 (1980) 585;
AI.B. Zamolodchikov, Int. J. Mod. Phys. A 10 (1995) 1125;
J. Balogh, A. Hegedűs, J. Phys. A 33 (2000) 6543;
G.v. Gersdorf, C. Wetterich, Phys. Rev. B 64 (2001) 054513;
H. Bozkaya, M. Faber, A.N. Ivanov, M. Pitschmann, J. Phys. A 39 (2006) 2177;
M. Faber, A.N. Ivanov, J. Phys. A 36 (2003) 7839.
[43] A. De Col, V.B. Geshkenbein, G. Blatter, Phys. Rev. Lett. 94 (2005) 097001.
[44] G. Delfino, G. Mussardo, Nucl. Phys. B 516 (1998) 675;
Z. Bajnok, L. Palla, G. Takács, F. Wágner, Nucl. Phys. B 601 (2001) 503;
G.Zs. Tóth, J. Phys. A 37 (2004) 9631;
G. Takács, F. Wágner, Nucl. Phys. B 741 (2006) 353.